UDC 551.509.313:551.509.327:551.515.21

ITERATIVE SOLUTIONS TO THE STEADY-STATE AXISYMMETRIC BOUNDARY-LAYER EQUATIONS UNDER AN INTENSE PRESSURE GRADIENT

RICHARD A. ANTHES

National Hurricane Research Laboratory, Environmental Research Laboratories, NOAA, Miami, Fla.

ABSTRACT

Steady-state solutions to the complete axisymmetric Navier-Stokes equations are obtained by an iterative technique for an intense pressure-gradient force representative of the tropical cyclone. Solutions for the horizontal and vertical components of motion are compared for various horizontal and vertical mixing coefficients, drag coefficients, and Coriolis parameters. A multilevel model is used, and the results are compared with those from a simple one-level model.

1. INTRODUCTION

Because of the intense frictional convergence in the boundary layer and the rapid decrease of mixing ratio with height, the major water vapor convergence in tropical cyclones occurs in the lowest few kilometers. Thus, the frictionally induced vertical motion at the top of the planetary boundary layer becomes a close measure of this convergence (Miller 1962, Riehl and Malkus 1961). Approximate expressions relating this vertical motion to the mean steady-state tangential wind have been given by several investigators (e.g., Syoño 1951, Charney and Eliassen 1949, Ogura 1964, and Smith 1968). Kuo (1971) utilized an iterative procedure to obtain exact solutions to the equations of motion in the boundary layer of a maintained vortex without the Coriolis term.

In a theoretical study of the hurricane boundary layer, Rosenthal (1962) neglected lateral mixing and vertical advection and obtained analytic solutions to the linearized equations. Rosenthal found a decreasing depth of inflow toward the center, with the consequence that the vertical velocities near the center appeared too small. Miller (1965) utilized a quasi-time-dependent numerical model to obtain steady solutions under various formulations of horizontal and vertical mixing and found that an inflow layer of constant depth could be obtained if the vertical mixing coefficient were made proportional to the pressure gradient.

In this paper, steady-state solutions to the axisymmetric boundary-layer equations are obtained by a numerical technique similar to Miller's (1965), with particular applicability to the boundary layer in hurricanes. The results are compared with those obtained by Kuo (1971) from a different approach. The results obtained from the equations of motion in primitive form are useful in interpreting results from more complex hurricane models, as well as providing lower boundary conditions on the mass transport required in diagnostic models such as Barrientos (1964) or Anthes (1970*b*).

In the experiments discussed here, the complete equations of motion are solved numerically for the horizontal and vertical velocity components under a steady, intense pressure-gradient force to study the effects of the variations of horizontal and vertical mixing, drag coefficients, and Coriolis parameter on the vertical motion at the top of the boundary layer. A multilevel model is used, and the results are compared with those obtained with a simple one-level model. This is a relevant comparison in view of the use of low vertical resolution boundary layers in hurricane models.

2. A MULTILEVEL BOUNDARY LAYER MODEL

A. BASIC EQUATIONS

When assuming axisymmetry and a pressure-gradient force invariant with height, the equations of motion for the tangential, v, and radial, u, winds are

$$\frac{\partial rv}{\partial t}=-u\frac{\partial rv}{\partial r}+r\left\{-w\frac{\partial v}{\partial z}-fu+\frac{\partial \mu\frac{\partial v}{\partial z}}{\partial z}+\frac{1}{r^2}\frac{\partial\left[Kr^3\frac{\partial v/r}{\partial r}\right]}{\partial r}\right\} \tag{1}$$

and

$$\frac{\partial u}{\partial t}=-u\frac{\partial u}{\partial r}-w\frac{\partial u}{\partial z}+fv+\frac{v^2}{r}-\frac{1}{\rho}\frac{\partial p}{\partial r}+\frac{\partial \mu\frac{\partial u}{\partial z}}{\partial z}+\frac{1}{r^2}\frac{\partial\left[Kr^3\frac{\partial u/r}{\partial r}\right]}{\partial r} \tag{2}$$

where w is vertical velocity, r is radial distance, z is height, f is the Coriolis parameter, ρ is mean density (1.1×10^{-3} gm·cm^{-3}), p is pressure, and K and μ are the horizontal and vertical coefficients of eddy viscosity, respectively. The continuity equation, neglecting density variations, is

$$\frac{\partial w}{\partial z}=-\frac{1}{r}\frac{\partial(ru)}{\partial r}. \tag{3}$$

B. STRUCTURE OF MODEL

The model consists of nine levels in the vertical defined by

$$z_i=50\text{ m}+(9-i)\Delta z \quad (\Delta z=100\text{m}, i=1,2, \ldots,9)$$

and 51 increments in the radial direction defined by

$$r_j=(j-1)\Delta r \quad (\Delta r=10\text{km}, j=1,2, \ldots,51).$$

The horizontal boundary conditions are zero divergence and relative vorticity at 500 km. These conditions have given reasonable solutions for multilevel hurricane models (Rosenthal 1970, Anthes 1970*a*) and should be representative of the hurricane environment at this distance from the center. The vertical boundary conditions consist of the tangential flow in gradient balance at the upper level with zero radial velocity. These conditions for the top of the Ekman layer are reasonable for the hurricane, which is in near-gradient balance at this level (Hawkins and Rubsam 1968). At the lowest level (50 m), the vertical velocity is assumed equal to zero. Boundary conditions on the vertical mixing term at the surface are

$$\mu\frac{\partial v}{\partial z}=C_D|\mathbf{V}|v$$

and (4)

$$\mu\frac{\partial u}{\partial z}=C_D|\mathbf{V}|u$$

where C_D is the drag coefficient and $\mathbf{V}$ is the vector velocity. The eq (4) are the well-known quadratic stress law.

The choice of the vertical and horizontal resolutions and the top level of 850 m was made after a series of preliminary experiments in which these computational aspects of the model were investigated. These results showed that increasing the horizontal and vertical resolutions beyond 10 km and 100 m, respectively, did not substantially alter the steady-state solutions. They also showed that, under the upper level boundary condition of gradient balance, increasing the top level beyond 850 m had little effect on the solutions.

C. COMPUTATIONAL PROCEDURE AND INITIAL CONDITIONS

Several finite-difference analogs to eq (1) and (2) are solved iteratively under a steady pressure-gradient force. The horizontal grid is staggered so that v and u are predicted at integer multiples of Δr with w computed diagnostically at points midway between u points according to

$$\frac{w_{i-1,j}-w_{i,j}}{\Delta z}=-\frac{r_{j+1}(u_{i,j+1}+u_{i-1,j+1})-r_j(u_{i,j}+u_{i-1,j})}{2r_{j+\frac{1}{2}}\Delta r}. \quad (5)$$

The initial conditions, or first guess, are the tangential wind in gradient balance with zero radial and vertical velocity. The eq (1) and (2) are forecast [1] utilizing several finite-difference schemes (to be discussed later) until the difference between successive iterates becomes small (less than 10^{-2} cm·s^{-1}). This usually occurs after about 400 iteration steps. The gradient wind corresponding to the specified pressure-gradient force is shown in figure 1.

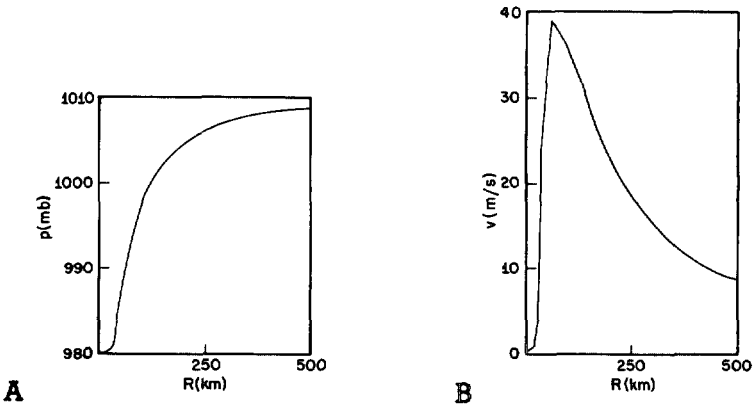

FIGURE 1.—(A) steady pressure profile and (B) the associated gradient wind at 20°N for the boundary-layer experiments.

The first series of experiments are computed utilizing the Matsuno (1966) time-integration scheme which damps high-frequency waves. Centered differences are used to approximate the space differentials in eq (1) and (2). The time step, Δt, is 90 s.

3. RESULTS

A. VARIATION OF HORIZONTAL AND VERTICAL EXCHANGE COEFFICIENTS

Values of K and μ ranging over several orders of magnitude have been used by previous investigators for the hurricane problem (Anthes 1970*a*), and values that give realistic results (compared to observations) in a particular instance are functions of the type of model, the horizontal and vertical resolution, and finite-difference scheme utilized. Unfortunately, the results are strongly dependent on the poorly understood process of horizontal and vertical diffusion of momentum. The first set of experiments, therefore, considers various constant horizontal and vertical exchange coefficients.

Figure 2 shows the steady-state vertical motion cross-sections for μ equal to 40 and three values of K ranging from 5 to 25 (units of μ and K are 10^4 and 10^8 cm^2·s^{-1} throughout the paper). Although the vertical motion structures for the three values of K are quite similar beyond the radius of maximum wind (R_{max}=50 km), significant differences are present inside the 50-km radius. The maximum upward motion ranges from 70 cm/s for

[1] The term "forecast" is used here as in time-dependent forecast models in which the pressure field is free to interact with the momentum field. In these experiments, in which the pressure is steady, the transient solutions have little physical meaning, and the forecast steps are more properly called "iteration steps."

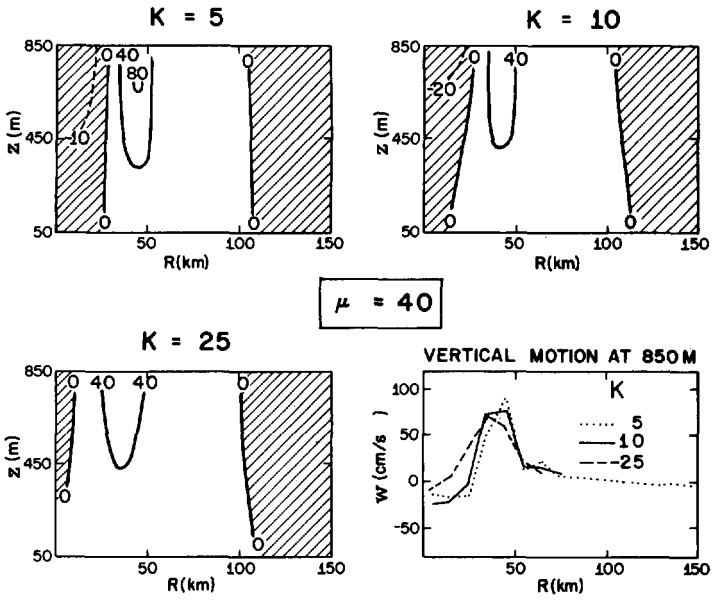

FIGURE 2.—Steady-state vertical motion for three horizontal mixing coefficients; units of K, 10^8 cm^2·s^{-1}; units of μ, 10^4 cm^2·s^{-1}; units of vertical motion isolines, cm/s.

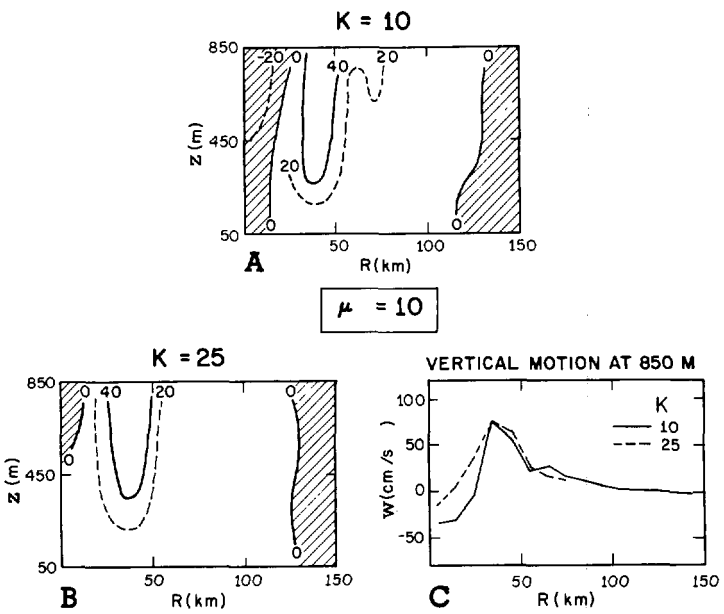

FIGURE 3.—Vertical motion for two horizontal mixing coefficients and a vertical mixing coefficient of 10×10^4 cm^2·s^{-1}; units of vertical motion isolines, cm/s.

$K=25$ to 91 cm/s for $K=5$. The subsidence near the center also shows strong dependence on horizontal mixing. For values of $K<25$, this subsidence results from a mixing of tangential momentum into the "eye," causing an excess of centripetal over pressure-gradient force and an outward flow. For very large values of K, however, the tangential wind maximum is reduced, and the mixing of radial momentum is sufficient to allow inflow all the way to the center. The subsidence associated with the smaller values of K reaches all the way to the surface and appears somewhat too large. Observations inside hurricane eyes generally show some low-level clouds, indicating that subsidence probably does not extend to the surface. This consideration suggests that a value of $K=25$ gives most realistic results for *this* model.

The values of K considered in the above experiments are higher than values used by previous investigators, a consequence perhaps of the differences in types of model, numerical scheme, and resolution noted above. If horizontal mixing is an important process in the vicinity of the radius of maximum wind, however, a simple scale analysis suggests values of this order of magnitude. For example, if the order of magnitude of the horizontal mixing term is equated to the magnitude of the centripetal term

$$K\frac{\Delta u}{\Delta r^2}\sim\frac{v^2}{r}$$

and

$v=30$ m/s, $r=50$ km, $\Delta r=10$ km, and $\Delta u=10$ m/s,

the magnitude of K is about 20×10^8 cm^2·s^{-1}.

Figure 3 shows vertical motion cross-sections for μ reduced from 40 to 10. The results show a more shallow layer of stronger radial velocities and more vertical shear. The subsidence inside R_{max} is reduced as the stronger inflow reaches closer to the origin. The transition from upward to downward motion is shifted from 115 km to 135 km as μ is reduced. The results also show more horizontal irregularities in vertical motion for small values of K (fig. 3C). These horizontal oscillations are apparently computational in nature and are related to nonlinear instability. Many experiments with a one-level model (Anthes 1970*a*) utilizing the same differencing scheme have shown these standing space oscillations of wavelength $2\Delta r$, which, for small values of K, may grow and prevent a steady-state solution. The computational nature of these oscillations is indicated by their strong dependence on time and space differencing and on horizontal resolution.

Figure 4 shows the boundary-layer structure for the tangential and radial winds for typical values of K and μ. Figure 4A, when compared to figure 1B, shows a region of subgradient winds beyond the radius of maximum wind due to surface friction, and a region of supergradient winds near the radius of maximum wind due to the strong radial advection of angular momentum inward. The radial velocities show a maximum of over 20 m/s just above the surface. The radial and tangential components are thus the same order of magnitude in the lower levels. Rosenthal (1969) found inflow angles greater than 45° in a hurricane model. While this magnitude is larger than those generally observed, Rosenthal notes that aircraft observations are probably above the level of maximum inflow.

418-596 O - 71 - 2

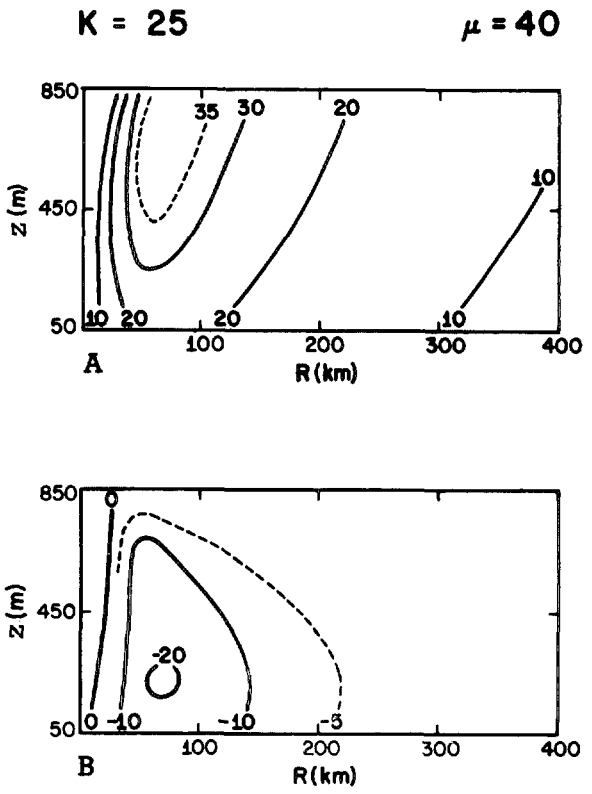

FIGURE 4.—Boundary-layer structures for (A) tangential and (B) radial wind components; units of K, 10^8 cm^2·s^{-1}; units of μ, 10^4 cm^2·s^{-1}; units of velocity component isolines, m/s.

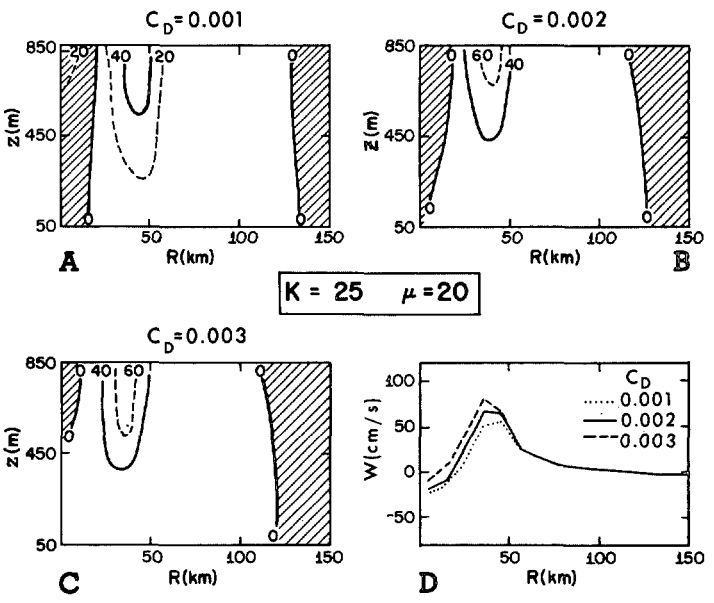

FIGURE 5.—Vertical motion for various drag coefficients; units of K, 10^8 cm^2·s^{-1}; units of μ, 10^4 cm^2·s^{-1}; units of vertical motion isolines, cm/s.

The trend for smaller vertical mixing toward stronger, more shallow inflow, weaker subsidence inside R_{max}, and larger transitional radius between upward and downward motion is investigated by a further reduction in μ from 10 to 5. The results (not shown) confirm the above tendencies, as the inflow increases from 27.5 to 29.3 m/s, the subsidence inside R_{max} is reduced, and the transitional radius from upward to downward motion shifts outward from 135 to 145 km.

In summarizing the effects of horizontal and vertical mixing, the maximum upward motion near the radius of maximum wind and also the subsidence inside this radius increase with decreasing values of K. The results are less sensitive to variations in μ, with higher values of μ yielding less vertical shear, a deeper inflow layer, and slightly increased vertical motion.

B. VARIATION OF DRAG COEFFICIENT

Although empirical evidence suggests a linear increase of drag coefficient with wind speed (Miller 1964), many investigators have utilized a constant drag coefficient in hurricane studies (Yamasaki 1968, Rosenthal 1969, Anthes 1970*a*). Figure 5 shows vertical motion structures for constant values of C_D ranging from 0.001 to 0.003. The results beyond 50 km are insensitive to variations in C_D. Inside 50 km, the maximum upward motion increases, and the subsidence decreases for increasing C_D, due to increased radial winds that penetrate closer to the axis. These results illustrate the paradox of the dual role of surface friction, with increased friction yielding more intense circulations for the range of drag coefficients considered.

C. VARIATION OF CORIOLIS PARAMETER

In this subsection, the Coriolis parameter is varied from 12.6×10^{-5} s^{-1} (corresponding to 60°N) to zero. For the constant pressure-gradient force, therefore, the gradient wind maximum varies from 36.9 m/s at 60 km (for 60°N) to 40.5 m/s at 65 km ($f=0$). The horizontal and vertical exchange coefficients are 25 and 5, respectively.

Figure 6 shows the vertical motion profiles for various values of f. As f decreases, the vertical motion maximum increases, the region of subsidence inside R_{max} disappears, and the area of rising motion expands outward. For the smaller values of f, the conversion of radial to tangential momentum decreases, and the inflow penetrates closer to the origin. For $f=0$, in fact, the tangential equation of motion becomes linearly uncoupled with the radial equation of motion, and no conversion from radial to tangential motion is possible. However, the radial equation is still strongly coupled to the tangential equation through the centripetal acceleration v^2/r. This strong coupling in one direction and weak coupling in the other makes the convergence to a steady state slower when f is small. Convergence is especially slow inside R_{max}, where the nonlinear coupling through vertical and horizontal advection is small and v^2/r is very large. In fact, the solutions do not converge to a steady state at all in this region when other

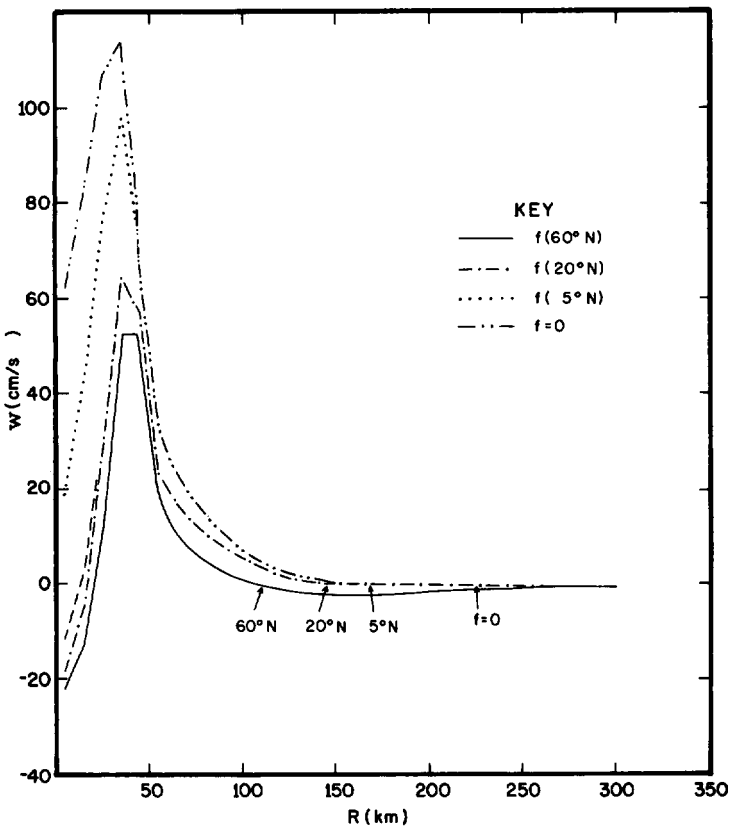

FIGURE 6.—Vertical motion at the top of the boundary layer for various latitudes.

integration schemes that do not damp the high frequencies are used (see appendix).

Further computational difficulties involving the nonlinear vertical mixing term and the upper boundary condition of gradient balance appear for very small f. For certain values of μ, vertical oscillations in u and v appear near the top of the boundary layer inside R_{max}. While the upper boundary condition of gradient balance appears realistic beyond R_{max} where horizontal mixing is unimportant, this condition yields unreasonable vertical shear inside R_{max} where horizontal mixing produces large cyclonic winds below the upper boundary. In the presence of the linear Coriolis coupling between the tangential and radial equations of motion, a balance is established in spite of this large shear. Without the Coriolis force, however, vertical oscillations develop near the upper boundary.

The experiment with $f=0$ corresponds to the case treated by Kuo (1971); although in Kuo's work, the vertical and horizontal exchange coefficients are equal. Because of this fact and the different nature of the approaches, quantitative comparisons are difficult. Qualitatively, the results are in fairly good agreement, depending on which value of the parameter K in Kuo's paper is considered. Both results show weak descending motion in the outer region with strong rising motion with a sharp

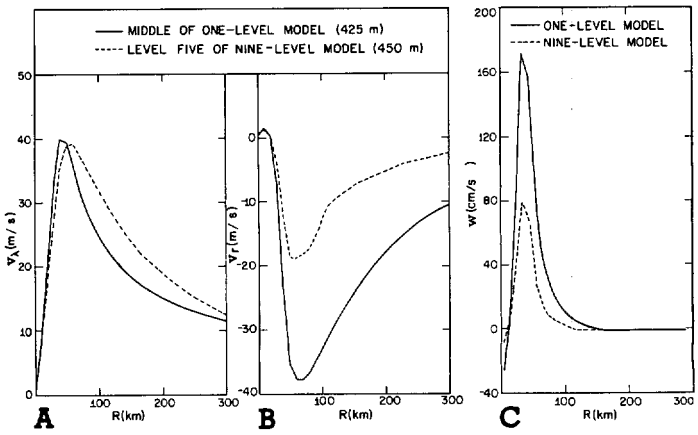

FIGURE 7.—Tangential and radial wind profiles in the middle of the nine-level and one-level models and the vertical motion profiles at the top of the nine-level and one-level models; V_λ is tangential velocity.

maximum in the vicinity of R_{max}. The vertical oscillations of the v and u profiles inside R_{max}, which were found by Kuo for small values of K, are not observed in this experiment, due possibly to the large values of vertical and horizontal mixing coefficients.

D. COMPARISON OF NINE-LEVEL MODEL RESULTS WITH ONE-LEVEL MODEL RESULTS

Since hurricane models (Ooyama 1969, Yamasaki 1968, Rosenthal 1970) contain one-level boundary layers, it is interesting to compare the results from the multilevel boundary-layer model with results from a simple one-layer model used by Anthes (1970*a*) in a similar series of experiments. In this model, u and v are calculated at the center of a boundary layer of constant depth, a linear variation of stress with height is assumed, and vertical advection is neglected.

Figure 7 compares the tangential and radial wind profiles at the center of the multilevel and one-level models and the corresponding vertical motion profiles at the top of the boundary layer. In both models, $K=25$; and in the multilevel model, $\mu=20$. It is evident from figure 7 that the effect of surface friction is overestimated by the one-level model. The tangential winds are less in the one-level model, and the radial velocities and vertical motion are larger by a factor of 2. This overestimation of the radial winds is probably a result of the assumption of linear stress over the boundary layer of constant depth. In the multilevel model, the stress varies strongly near the surface and less strongly throughout the upper part of the boundary layer.

E. BALANCE OF FORCES IN THE STEADY STATE

An estimate of the balance of forces in various regions of the domain may be made by comparing the various terms in eq (1) and (2) in the steady state. Table 1 shows

TABLE 1.—*Ratio of terms in the radial equation of motion to the pressure-gradient force in the steady state; $K=25\times10^6$ cm^2·s^{-1}; $\mu=20\times10^4$; and $\epsilon<0.1$.*

R	$\frac{1}{\rho}\frac{\partial p}{\partial r}$	Ratio of term to pressure-gradient force					
		$u\frac{\partial u}{\partial r}$	$w\frac{\partial u}{\partial z}$	fv	v^2/r	Vertical mixing	Horizontal mixing
(km)	(cm·s^{-2})			$z=750$ m			
10	0.0014	−17.6	−6.5	21.7	263.0	−193.0	− 66.9
20	.0066	− 0.5	44.2	11.6	176.0	−106.0	−124.0
30	.0733	1.0	−1.9	1.9	36.3	− 11.4	− 24.9
40	1.56	− .18	−1.7	.12	2.2	0.33	0.23
50	3.16	ϵ	− .88	ϵ	1.01	.41	.45
100	1.50	ϵ	ϵ	.12	.83	ϵ	ϵ
200	.37	ϵ	ϵ	.30	.65	ϵ	ϵ
400	.081	ϵ	ϵ	.63	.33	ϵ	ϵ
				$z=150$ m			
10	0.0014	−10.5	−9.5	26.9	404.0	41.8	−452.0
20	.0066	−21.8	−6.0	11.4	169.0	21.8	−174.0
30	.0733	− 9.4	− .5	1.5	21.1	3.9	− 15.6
40	1.56	− 0.9	ϵ	ϵ	1.1	.3	0.3
50	3.16	− .3	ϵ	ϵ	.5	.2	.5
100	1.50	.2	ϵ	ϵ	.3	.3	ϵ
200	.37	.1	ϵ	.2	.3	.4	ϵ
400	.081	ϵ	ϵ	.5	.2	.4	ϵ

TABLE 2.—*Qualitative effect of varying parameters on significant features of the vertical motion structure in the boundary layer*

Parameter	Feature		
	Subsidence inside R_{max}	Vertical motion maximum	Transitional radius from upward to downward motion
K	Decreases	Decreases	------
μ	------	Increases	Decreases
C_D	Decreases	Increases	------
f	Increases	Decreases	Decreases

Increases in the above parameters are accompanied by the given effect on the features of the vertical motion structures; the dashed lines indicate no appreciable effect.

the ratio of the terms in eq (2) to the pressure-gradient force for a typical experiment. From table 1, it is clear that no term, with the possible exception of the vertical advection term, may be neglected over the entire domain. Very close to the center, the centripetal acceleration nearly balances the horizontal and vertical mixing. The importance of horizontal mixing falls off rapidly with increasing distance and is relatively unimportant beyond 100 km. Vertical advection is important only near R_{max}. The relative importance of the Coriolis force increases with increasing distance. Horizontal advection and surface drag are important at all distances. The boundary layer, then, consists of an inner region where horizontal mixing and centripetal acceleration are dominant, an intermediate region in the vicinity of R_{max} where all terms are significant, and an outer region where vertical advection and horizontal mixing are unimportant.

4. SUMMARY

The quantitative results from this series of experiments investigating the boundary-layer structure under a steady, intense pressure gradient are difficult to summarize, mainly because the numerical values are strongly dependent on the parameters K, μ, f, and C_D as well as on vertical resolution and upper and lateral boundary conditions. The qualitative results are therefore summarized briefly in table 2. Thus, subsidence inside R_{max} is favored by small values of K and large values of f; the vertical motion maximum increases as drag friction and vertical mixing increase, and the area of rising motion increases for small μ and small f.

The results from the multilevel model are compared with the results from a one-level model. Although the conclusions based on experiments using the one-level model (Anthes 1970*a*) are not changed, the one-level model appears to overestimate the radial and vertical motions in comparison to the multilevel results, due primarily to the assumption of a linear stress boundary layer of constant depth.

Most experiments are carried out with the Matsuno (1966) scheme that damps high frequencies. Comparative experiments with other schemes show similar results when the Coriolis term is large. However, for small values of f, the schemes without the high-frequency damping do not converge to a steady state.

APPENDIX

RESULTS FROM TWO ADDITIONAL FINITE-DIFFERENCE SCHEMES

For assessing some of the computational effects on the solutions, two additional finite-difference schemes are tested for the model. The two-step Lax-Wendroff (1960) time-integration scheme has second-order accuracy but contains some damping, especially for short wavelengths (Richtmyer 1963). One cycle of this scheme, which is twice as fast as the Matsuno scheme, is summarized for $\partial\alpha/\partial t=F(\alpha)$:

1. Given $\alpha^n_{i,j}$.
2. Compute the first step from

$$\alpha^{n+1}_{i,j}=\frac{1}{4}(\alpha_{i-1,j}+\alpha^n_{i+1,j}+\alpha^n_{i,j+1}+\alpha^n_{i,j-1})+\Delta tF(\alpha^n).$$

3. Compute the final step from

$$\alpha^{n+2}_{i,j}=\alpha^n_{i,j}+2\Delta tF(\alpha^{n+1}_{i,j}).$$

The space derivatives in eq (1) and (2) are evaluated with centered differences.

The other scheme tested is the popular forward-time upstream space-differencing scheme, which is also twice as fast as the Matsuno scheme. This scheme has only first-order accuracy and contains strong damping of short wavelengths, but nevertheless has given excellent results in hurricane modeling experiments (Rosenthal 1970).

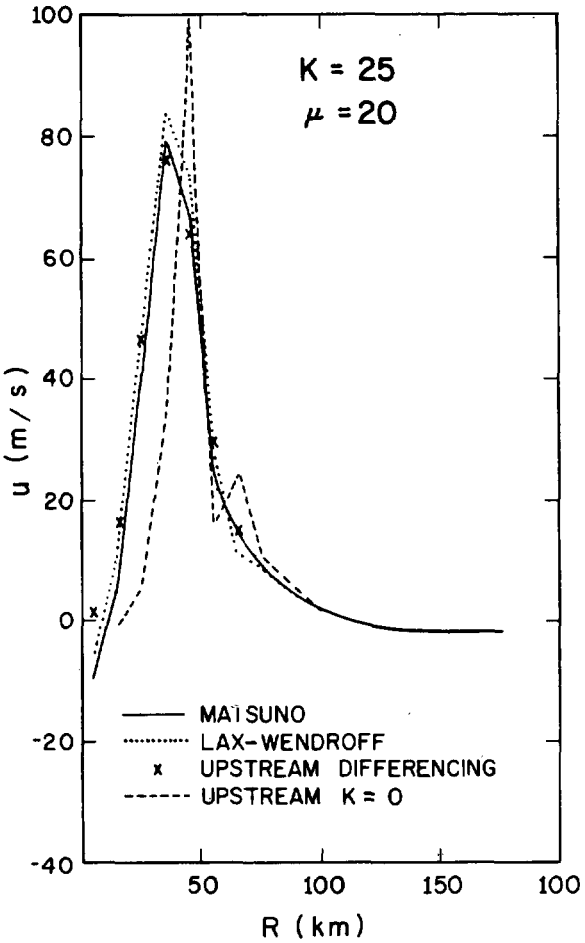

FIGURE 8.—Comparison of three integration schemes used to compute steady-state vertical velocity profiles at the top of the boundary layer for $K=25\times10^8$ cm^2·s^{-1} and $\mu=20\times10^4$ cm^2·s^{-1}. Also shown is the vertical velocity profile computed from forward-time upstream space-differencing with no explicit mixing ($K=0$).

The steady-state solutions to the boundary-layer equations are computed for values of $K=25$ and $\mu=20$ for all three schemes. Figure 8 shows the vertical velocity profiles at the top of the boundary layer for the three experiments. The results are very nearly the same, indicating that the explicit damping is dominating the different damping properties of the three schemes. The only significant difference is the absence of subsidence near the origin in the upstream-differencing experiment. The large space truncation present in the upstream-differencing technique provides a pseudodiffusive effect (Molenkamp 1968, Rosenthal 1970, Orville and Sloan 1970) that allows steady-state solutions even with no explicit horizontal diffusion. With either the Matsuno or Lax-Wendroff schemes, however, steady-state solutions are not obtained for $K=0$. Figure 8 shows the vertical velocity profile for upstream differencing with $K=0$. The artificial damping yields reasonable solutions beyond the radius of maximum wind. However, this pseudodiffusion does not simulate the effect of horizontal mixing by eddy coefficients inside the radius of maximum wind, as shown by the absence of subsidence. The pseudodiffusion depends on truncation in the advection terms. Inside the radius of maximum wind, the radial advection is small, so there is little implicit mixing, even though the curvatures of the tangential and radial wind profiles are large. The subsidence, which depends on mixing of cyclonic momentum inward from the radius of maximum wind, is not present in the upstream-differencing experiments with no explicit mixing. This difference is also present in experiments with a one-level boundary layer model (Anthes 1970*a*).

Although steady-state solutions that are not too different from each other are obtained from the three integration schemes tested for a value of the Coriolis parameter equal to 5×10^{-5} s^{-1} (20°N), steady-state solutions for smaller values of f are not obtained from either the Lax-Wendroff or the forward-time integrations. For small values of f (see subsection C of section 2), the high-frequency damping in the Matsuno scheme is necessary for convergence to a steady state.

ACKNOWLEDGMENTS

The author expresses his appreciation to Drs. Banner I. Miller and Stanley L. Rosenthal for their helpful comments concerning this research and to Prof. H. L. Kuo for his careful review of the manuscript.

REFERENCES

Anthes, Richard Allen, "A Diagnostic Model of the Tropical Cyclone in Isentropic Coordinates," *ESSA Technical Memorandum* ERLTM-NHRL 89, U.S. Department of Commerce, National Hurricane Research Laboratory, Miami, Fla., Apr. **1970***a*, 147 pp.

Anthes, Richard Allen, "The Role of Large-Scale Asymmetries and Internal Mixing in Computing Meridional Circulations Associated With the Steady-State Hurricane," *Monthly Weather Review*, Vol. 98, No. 7, July **1970***b*, pp. 521–528.

Barrientos, Celso S., "Computations of Transverse Circulation in a Steady State, Symmetric Hurricane," *Journal of Applied Meteorology*, Vol. 3, No. 6, Dec. **1964**, pp. 685–692.

Charney, Jule G., and Eliassen, Arnt, "A Numerical Method for Predicting the Perturbations in the Middle-Latitude Westerlies," *Tellus*, Vol. 1, No. 2, Stockholm, Sweden, May **1949**, pp. 38–54.

Hawkins, Harry F., and Rubsam, Daryl T., "Hurricane Hilda, 1964: II. Structure and Budgets of the Hurricane on October 1, 1964," *Monthly Weather Review*, Vol. 96, No. 9, Sept. **1968**, pp. 617–636.

Kuo, H. L., "Axisymmetric Flows in the Boundary Layer of a Maintained Vortex," *Journal of the Atmospheric Sciences*, Vol. 28, No. 1, Jan. **1971**, pp. 20–41.

Lax, Peter D., and Wendroff, Burton, "Systems of Conservation Laws," *Communications on Pure and Applied Mathematics*, Vol. 13, Interscience Publications, Inc., New York, N.Y., **1960**, pp. 217–237 (see p. 217).

Matsuno, Taroh, "Numerical Integrations of the Primitive Equations by a Simulated Backward Difference Method," *Journal of the Meteorological Society of Japan*, Ser. 2, Vol. 44, No. 1, Tokyo, Feb. **1966**, pp. 76–84.

Miller, Banner I., "On the Momentum and Energy Balance of Hurricane Helene (1958)," *National Hurricane Research Project Report* No. 53, U.S. Department of Commerce, Weather Bureau, Miami, Fla., Apr. **1962**, 19 pp.

Miller, Banner I., "A Study of the Filling of Hurricane Donna (1960) Over Land," *Monthly Weather Review*, Vol. 92, No. 9, Sept. **1964**, pp. 389–406.

Miller, Banner I., "A Simple Model of the Hurricane Inflow Layer," *Weather Bureau Technical Note* 18—NHRL 75, U.S. Department of Commerce, National Hurricane Research Laboratory, Miami, Fla., Nov. **1965**, 16 pp.

Molenkamp, Charles R., "Accuracy of Finite Difference Methods Applied to the Advection Equation," *Journal of Applied Meteorology*, Vol. 17, No. 2, Apr. **1968**, pp. 160–167.

Ogura, Yoshimitsu, "Frictionally Controlled, Thermally Driven Circulations in a Circular Vortex With Application to Tropical Cyclones," *Journal of the Atmospheric Sciences*, Vol. 21, No. 6, Nov. **1964**, pp. 610–621.

Ooyama, Katsuyuki, "Numerical Simulation of the Life-Cycle of Tropical Cyclones," *Journal of the Atmospheric Sciences*, Vol. 26, No. 1, Jan. **1969**, pp. 3–40.

Orville, H. D., and Sloan, L. J., "Effects of Higher Order Advection Techniques on a Numerical Cloud Model," *Monthly Weather Review*, Vol. 98, No. 1, Jan. **1970**, pp. 7–13.

Richtmyer, Robert D., "A Survey of Difference Methods for Non-Steady Fluid Dynamics," *NCAR Technical Notes* 63–2, National Center for Atmospheric Research, Boulder, Colo., **1963**, 25 pp.

Riehl, Herbert, and Malkus, Joanne S., "Some Aspects of Hurricane Daisy, 1958," *Tellus*, Vol. 13, No. 2, Stockholm, Sweden, May **1961**, pp. 181–213.

Rosenthal, Stanley L., "A Theoretical Analysis of the Field of Motion in the Hurricane Boundary Layer," *National Hurricane Research Project Report* No. 56, U.S. Department of Commerce, Weather Bureau, Miami, Fla., June **1962**, 12 pp.

Rosenthal, Stanley L., "Numerical Experiments With a Multilevel Primitive Equation Model Designed to Simulate the Development of Tropical Cyclones: Experiment I," *ESSA Technical Memorandum* ERLTM–NHRL 82, U.S. Department of Commerce, National Hurricane Research Laboratory, Miami, Fla., Jan. **1969**, 36 pp.

Rosenthal, Stanley L., "Experiments With a Numerical Model of Tropical Cyclone Development—Some Effects of Radial Resolution," *Monthly Weather Review*, Vol. 98, No. 2, Feb. **1970**, pp. 106–120.

Smith, R. K., "The Surface Boundary Layer of a Hurricane," *Tellus*, Vol. 20, No. 3, Stockholm, Sweden, **1968**, pp. 473–484.

Syoño, Sigekata, "On the Structure of Atmospheric Vortices," *Journal of Meteorology*, Vol. 8, No. 2, Apr. **1951**, pp. 103–110.

Yamasaki, Masanori, "Numerical Simulation of Tropical Cyclone Development With the Use of Primitive Equations," *Journal of the Meteorological Society of Japan*, Vol. 46, No. 3, Tokyo, June **1968**, pp. 178–201.

[Received June 3, 1970; revised November 2, 1970]